Carbon monoxide bands in M dwarfs

Y. V. Pavlenko[1] and H. R. A. Jones[2]

[1] Main Astronomical Observatory of Academy of Sciences of Ukraine, Golosiiv woods, Kyiv-127, 03680 Ukraine
e-mail: yp@mao.kiev.ua
[2] Astrophysics Research Institute, Liverpool John Moores University, Egerton Wharf, Birkenhead CH41 1LD, UK
e-mail: hraj@astro.livjm.ac.uk

Abstract. We compare the observational and theoretical spectra of the $\Delta v = 2$ CO bands in a range of M dwarfs. We investigate the dependence of theoretical spectra on effective temperatures as well as carbon abundance. In general we find that the synthetic CO bands fit the observed data extremely well and are excellent diagnostics. In particular the synthetic spectra reasonably match observations and the best fit temperatures are similar to those found by empirical methods. We also examine the $^{12}C/^{13}C$ isotopic ratio. We find that fundamental ^{13}CO bands around 2.345 and 2.375 μm are good discriminators for the $^{12}C/^{13}C$ ratio in M dwarfs. The 2.375 μm band is more useful because it doesn't suffer such serious contamination by water vapour transitions. Our current dataset does not quite have the wavelength coverage to perform a reliable determination of the $^{12}C/^{13}C$ ratio in M dwarfs. For this we recommend observing the region 2.31–2.40 μm at a resolution of better than 1000. Alternatively the observational problems of contamination by water vapour at 2.345 μm maybe solved by observing at resolutions of around 50 000. We also investigated the possibility of using the $\Delta v = 1$ CO bands around 4.5 μm. We find that the contamination due to water vapour is even more of a problem at these wavelengths.

Key words. stars: fundamental parameter

1. Introduction

More than 70% of stars in the vicinity of the Sun are M dwarfs. These numerous low-mass stars ($0.08\ M_\odot \leq M < 0.6\ M_\odot$), together with substellar objects – brown dwarfs ($M \leq 0.08\ M_\odot$) can contain an appreciable amount of the baryonic matter in the Galaxy. Research of M dwarf spectra are of interest for many branches of modern astrophysics. Verification of the theory of stellar evolution and structure of stars, the detection among M dwarfs of a subset of young brown dwarfs, the physical state of plasma of their atmospheres at low temperatures, as well as the chemical and physical processes of dust formation are only a few of them.

The dominant opacity sources in the optical and IR spectra of M dwarfs is absorption by band systems of diatomic molecules, such as TiO and VO, as well as rotational-vibrational bands of H_2O. M dwarf infrared spectra additionally contain absorption bands of CO. Apart from being readily identifiable in M dwarf spectra, CO bands have the advantage of being extremely well modelled. This is in contrast to the relatively poor modelling of other molecules and atomic lines in M dwarf atmospheres. For example, the structure of rotational-vibrational levels of two-nuclear molecules CO is much simpler, than H_2O. That allows computations of CO line lists to

be carried out with high accuracy (e.g., Goorvitch 1994). One of the most promising observational regions is located in the K band from 2.2 to 2.4 μm. Second overtone bands $^{12}C^{16}O$ and $^{13}C^{16}O$ are located here. As well as parameters such as effective temperature and gravity, they can be used for determination of carbon and/or oxygen abundances and the $^{12}C/^{13}C$ ratio in atmospheres of late-type stars. The determination of the $^{12}C/^{13}C$ ratio in M dwarf atmospheres is especially interesting. Following the conventional theory of stellar evolution (see Aller & McLaughlin 1965), M dwarfs save their initial $^{12}C/^{13}C$ from their time of formation. Since the galactic $^{12}C/^{13}C$ ratio is expected to change by around a factor of four over the lifetime of our Galaxy, the determination of the $^{12}C/^{13}C$ ratio for M dwarfs potentially gives a strong constraint on their age. However, determining the 12C/13C ratio is only a strong constraint on age if that ratio is a single-valued function of time and Galactic location. If that underlying assumption is not valid, any dispersion of $^{12}C/^{13}C$ in M-dwarf atmospheres might give for us some clues about mixing processes inside our Galaxy. Until now, measurements of the $^{12}C/^{13}C$ ratio for planetary nebulae, red giants and asymptotic giant branch stars do not fit particularly well with theory. Nonetheless, the discrepancies found for such evolved stars may well arise from the lack of realistic stellar models. Atmospheric models need to include additional physical processes in their prescription for mixing between nucleosynthetic cores and observable

atmospheres (Palla et al. 2000). M dwarfs, on the other hand, are not expected to modify their ^{12}C/^{13}C and are fully convective. Thus the ^{12}C/^{13}C ratios for a diverse sample of M dwarfs is expected to be a relatively straight-forward function of time and galactic location.

Until now studies of CO bands in the K-band were mainly used for the quantitative analysis of the evolution of ^{12}C/^{13}C in atmospheres of red giants (cf. Hinkle 1978; Sneden & Pilachowski 1984; McGregor 1987; Lazaro et al. 1991; Suntzeff & Smith 1992; Scott et al. 1994; Pilachovski et al. 1997). However, they are also observed in the spectra of many objects – from symbiotic stars (Schild et al. 1992), Be stars (Kraus et al. 2000) and supernova remnants (Gerardy et al. 2000) up to planets (Forbes et al. 1970). Baldwin et al. (1973) and many others since have shown the prevalence of the CO bands in the K band spectra of M dwarfs. Viti et al. (2002) have shown that the CO bands in the K band are relatively well-matched by synthetic spectra and thus can be used to determine M dwarf properties. In our study we make comparisons of synthetic and observed spectra across the 2.3–2.4 μm region to quantify the usefulness of the CO bands as a diagnostic of effective temperatures and metallicities for M dwarfs.

2. Observations

The properties of observed stars for which spectra are fitted in our paper are listed in Table 1. Observations were made with the Cooled Grating Spectrometer 4 on the UK Infrared Telescope (UKIRT) on Mauna Kea, Hawaii. The instrument then had a 58 × 62 InSb array which was moved in the focal plane in order to three times over-sample the spectrum. Sky subtraction was performed by nodding the telescope approximately 30 arcsec up and down the slit, ensuring that during alternate "object" and "sky" observations the star remained on the detector. The observations presented in this paper were made during three nights, 1992 May 8, 10 and 12 in reasonable optical seeing (0.75–1.5 arcsec) and of atmospheric humidity (10–50 per cent). The airmass difference between object and standard never exceeded 0.05 and so we are confident that the spectra have good cancellation of atmospheric features.

The 150 lines mm^{-1} grating was used in third order with the 150 mm focal length camera at a central grating wavelength of 2.34 μm. This grating position was chosen to be closed to the centre of the CO bands, at a maximum in the grating efficiency have high atmospheric transmission (>95 per cent) and gives a relatively high resolution, $\lambda/\Delta\lambda$, where $\Delta\lambda$ is the detector resolution at wavelength λ, of 1085 (equivalent to 276 km s^{-1}).

2.1. Standards

Stars in the spectral type ranges B5–A5 and F6–G0 were used to remove the effects of atmospheric absorption. These standards were expected to be featureless at the spectral resolution used and to be well described by a Rayleigh-Jeans tail. However, the F6–G0 standards were not very useful as they show weak metal lines. Although the lines tended to be weaker and different from the M dwarf features we avoided using them where possible. In the reduction of spectra, we have followed

the same procedures as in Jones et al. (1996). All observations were wavelength calibrated using lines from observations of an argon lamp in the CGS4 calibration unit. This procedure is typically accurate to 0.1 $\Delta\lambda$.

3. Procedure

We used local thermal equilibrium (LTE) model atmospheres of M dwarfs with effective temperatures T_{eff} = 2400–3800 K from the NextGen grid of Hauschildt et al. (1999). Unless otherwise mentioned all models are for log g = 5.0 and solar metallicity. Computations of LTE synthetic spectra were carried out by the program WITA6 (Pavlenko 2000) assuming LTE, hydrostatic equilibrium for an one-dimensional model atmosphere and without sources and sinks of energy. The equations of ionisation-dissociation equilibrium were solved for media consisting of atoms, ions and molecules. We took into account ~100 components (Pavlenko 2000). The constants for equations of chemical balance were taken from Tsuji (1973). We adopt the dissociation potential D_0 = 9.5 eV for H_2O and D_0 = 11.105 eV for ^{12}C^{16}O, ^{13}C^{16}O. It is worth noting that the chemical balance in M dwarf atmospheres is governed by the CO molecule (see Sect. 4.1).

Line lists of ^{1}H$_2^{16}$O were computed using the AMES database (Partrige & Schwenke 1998). The partition functions of H_2O were also computed on these data (Pavlenko 2002). We used ^{12}C^{16}O and ^{13}C^{16}O line lists of Goorvitch (1994). The CO partition functions were taken from Gurvitz et al. (1989). The atomic line list was taken from VALD (Kupka et al. 1999).

The profiles of molecular and atomic lines are determined using the Voigt function $H(a, v)$, parameters of their natural broadening C_2 and van der Waals broadening C_4 from databases (Kupka et al. 1999) or in their absence computed following Unsold (1955). Owing to the low temperatures in M dwarf atmospheres and consequently, electron densities, Stark broadening may be neglected. As a whole the effects of pressure broadening prevail. Computations for synthetic spectra were carried out with a resolution of 0.00005 μm for microturbulent velocity v_{t} = 2 km s^{-1}.

The instrumental broadening was modelled by triangular profiles set to the resolution of the observed spectra. To find the best fits to observed spectra we follow the scheme of Jones et al. (2002). Namely, for every spectrum we carry out the minimisation of a 3D function $S = f(x_{\text{s}}, x_{\text{f}}, x_{\text{w}}) = 1/N \times \sum(1 - F_{\text{obs}}/F_{\text{synt}})^2$, where $F_{\text{obs}}, F_{\text{synt}}$ are observed and computed fluxes, N is the number of points in observed spectrum to be fitted, $x_{\text{s}}, x_{\text{f}}, x_{\text{w}}$ are relative shift in wavelength scale, a normalisation factor which was used to coincide observed and computed spectra and parameter of instrumental broadening, respectively.

4. Results

4.1. CO and H$_2$O molecules in M dwarf atmospheres

The overall chemical balance in the atmospheres of cool stars depends significantly on the C/O = log N(C) − log N(O) (see Tsuji 1973). In the atmospheres of cool (T_{eff} < 3600 K) oxygen

Table 1. The properties of observed stars are taken from Jones et al. (1996). Spectral types are taken from Kirkpatrick et al. (1991).

Object	d (pc)	KIN	COL	Sp Type	M_K(CIT)	V_C–K_{CIT}	I_{CCD}–L'_{MKO}
Gl 411	2.5	OD	OD/H	dM2	6.34	4.11	2.24
Gl 699	2.39	OD/H	OD/H	dM4	8.20	5.04	2.59
Gl 406	1.83	OD	-	dM6	9.19	7.37	3.70
VB 10	5.79	OD	-	dM8	9.99	8.70	4.65
LHS 2924	10.72	OD	-	dM9	10.52	8.91	5.19

rich stars C/O < 0, almost all atoms of carbon are bound in CO molecules. CO and H_2O are the most abundant molecules containing oxygen atoms.

In the atmospheres of M dwarfs with T_{eff} > 2600 K, molecules of CO dominate by number in comparison with other oxygen containing molecules (Tsuji 1973). Throughout most of the atmosphere changes of the ratio C/O by ± 0.2 dex have little effect on the molecular densities of CO (Fig. 1). In contrast the dependence of molecular densities on H_2O on $\log N$ (C) is more complex. At lower T_{eff} (e.g. Fig. 1b) the dependence of n_{H_2O} on $\log N$(C) in M dwarfs atmospheres weakens appreciably though the chemical balance remains governed by CO. In general, H_2O and CO are competitors for bound-free oxygen atoms. Therefore their molecular densities respond in opposite ways to changes of carbon abundance. For solar abundances of oxygen and carbon, molecular densities of H_2O and CO are comparable. CO molecular densities increase only a little when $\log N$(C) increases from -3.48 up to -3.12[1]. At the same time CO reduces molecular densities of H_2O. However, relative changes of H_2O densities are comparatively weak for variations of $\log N$(C) in the range from -3.48 to -3.18. Only when the carbon abundance rises to $\log N$(C) $\sim$ -3.18, molecular densities of H_2O decrease, as an appreciable fraction of oxygen atoms become bound in CO.

The relative strengths of H_2O and CO bands at 2600 K and 3600 K are shown in Fig. 2. These spectra were computed separately by switching on/off the absorption of H_2O or CO bands.

The relative intensity of the CO bands decrease from $\Delta v = 1$ to $\Delta v = 3$. Although the second overtone bands ($\Delta v = 2$) of CO have intermediate intensities they are located in a relatively accessible region for observation.

4.1.1. Bands of the second overtone of CO from 2.28–2.4 μm

The relative intensities of $^{12}C^{16}O$ $^{13}C^{16}O$ and H_2O bands from 2.28–2.38 μm are shown in Fig. 3. These computations are carried out for a model atmosphere with 2600 K and $^{12}C/^{13}C = 0.5$. The large ratio of $^{12}C/^{13}C$ was chosen to show the positions of the main details which might be observed in M dwarf spectra. Overall, H_2O absorption dominates the infrared spectral region. However, strong features are also formed there by first overtone bands of $^{12}C^{16}O$. The positions of the $^{13}C^{16}O$ bandheads are marked by vertical arrows in Fig. 3. The results of our $^{13}C^{16}O$ modelling of spectra of our dwarfs are discussed in Sects. 4.1.3 and 4.1.4.

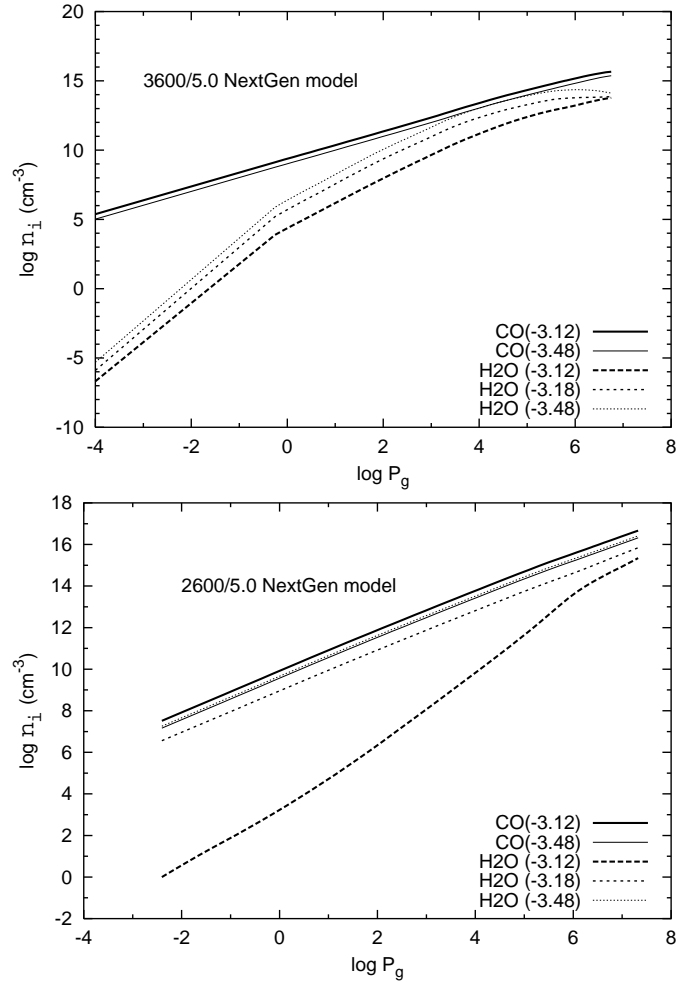[1] In our paper we use an abundance scale $\Sigma N_i = 1$.

Fig. 1. Molecular densities of H_2O and CO in atmospheres of M dwarfs 3600/5.0 and 2600/5.0 as a function of gas pressure P_g. The case of $\log N$(C) $= -3.48$ and $\log N$(O) $= -3.12$ represent the solar abundances case.

4.1.2. Fits to the observed spectra

Our numerical procedure for the determination of best fits allows us to quantify the possible solutions. For each observed spectra we compute synthetic spectra for different T_{eff}. We also allow for small variations of carbon abundances. Based on Fig. 1, we suggest that small variations of $\log N$(C) from -3.48 to -3.28 cannot substantially affect the temperature structure of the model atmospheres. From the family of curves $S = f(T_{eff}, \log N(C))$ we choose "the best solution" for each observed spectrum.

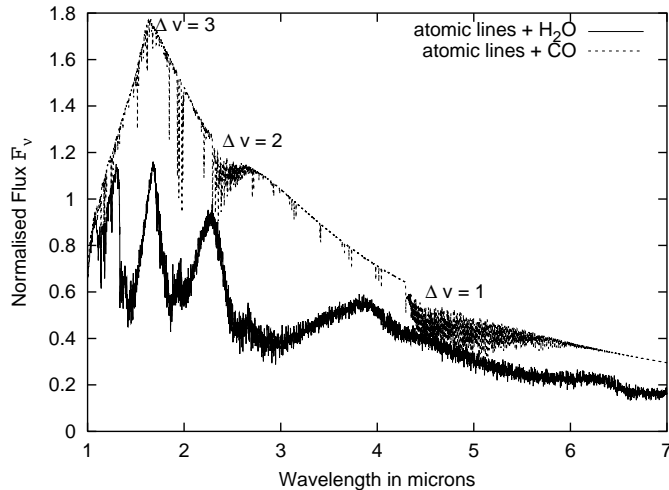**Fig. 2.** The relative strength of $^{12}C^{16}O$ and H_2O bands in a 2600 K synthetic spectrum. The positions and relative strengths of the CO bands can be seen.

LHS2924. The observed spectrum of this M9V object is of relatively low signal-to-noise. For example, our best fit minimisation value S_{min} for LHS2924 is a factor 10 larger than VB10 (Fig. 4). Our best fit provides T_{eff} = 2800 K for $\log N(C)$ = −3.28 and T_{eff} = 2600 K for a solar abundance of carbon ($\log N(C)$ = −3.48).

VB10. VB10 is an archetypal late-type M dwarf with an effective temperature $T_{eff} \sim$ 2600 K (Jones et al. 1996). Lithium lines are absent from VB10's spectrum (Schweitzer et al. 1996; Martin 1999) and it has typical old disk properties (Leggett 1992) and hence VB10 is a star right at the end of the main sequence. For the solar abundance of carbon and other elements S_{min} occurs for 2600 K. However, if we increase $\log N(C)$, S decreases, and we find a best fit value of 2800 K for $\log N(C)$ = −3.28 ± 0.1. In general, for higher $\log N(C)$, CO bands intensities increase and best fits move to higher T_{eff}. The same effect is found for all dwarfs of our sample.

GJ406. Best fits are found for 2800 K for the solar abundance case, and 3000 K for $\log N(C)$ = −3.28 (Fig. 6). Our new estimation of effective temperature corresponds better with empirical values for the effective temperature of the spectral class M6V than the Jones et al. (2002) analysis found using a similar technique but using a region dominated by water vapour. Our best fits for GJ406 are found for solar metallicity rather than the metal poor result found by Jones et al. (2002).

GJ699. The observed spectrum of GJ699 (M4V) is of lower resolution and taken from the setup used in Jones et al. (1994). The details in observed spectrum are best fit by metal-poor ($\log N(C)$ = −3.68; i.e., [C] = −0.2) synthetic spectra of T_{eff} = 3200 K (see Fig. 7). The same best fit temperature is also found for the solar abundances $\log N(C)$ = −3.48, ([C] = 0) case. However, a carbon-deficient case $\log N(C)$ = −3.68 ([C] = −0.2) provides lower S. We note that Jones et al. (2002) found an effective temperature T_{eff} = 3300 K and metallicity [M/H] = −0.5 ([O] = −0.5). On the other hand, our fits with $\log N(C)$ = −3.88 ([C] = −0.4) provide less satisfactory fits. i.e. fits of higher S. We have probably reached the limit at
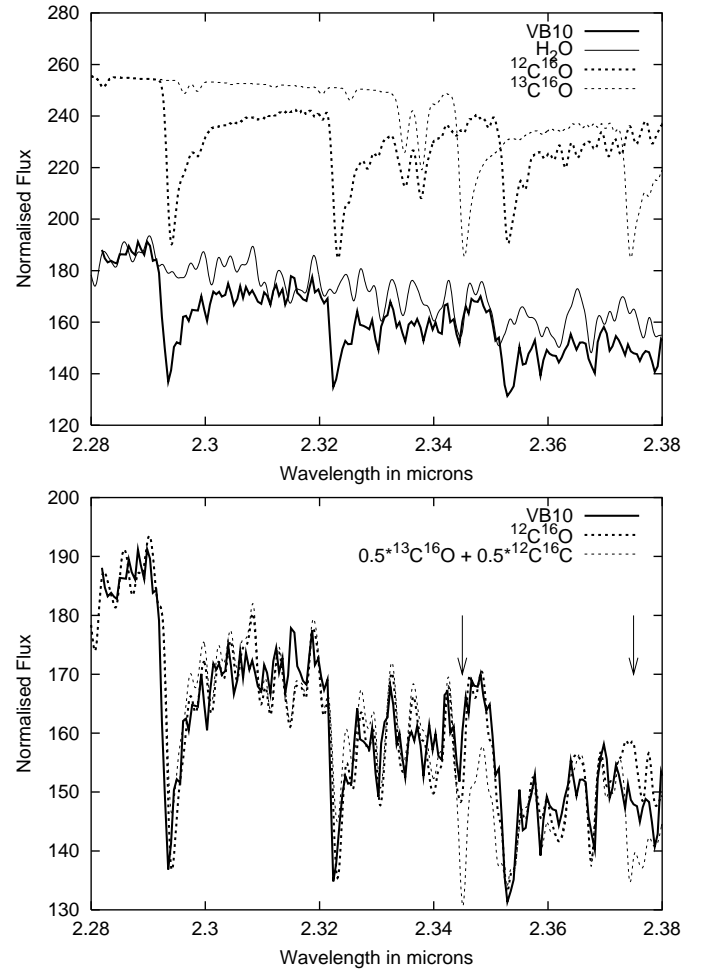

Fig. 3. The relative strength of $^{12}C^{16}O$, H_2O and $^{13}C^{16}O$ bands in the spectrum of VB10 (top), and a combined spectra computed for the case of $^{12}C^{16}O$ + H_2O and $^{12}C^{16}O$ + $^{13}C^{16}O$ + H_2O absorptions. The model atmospheres shown are 2600 K, $^{12}C/^{13}C$ = 0.5 (bottom). The positions of $^{13}C^{16}O$ bands heads are shown by arrows.

which a single metallicity parameter is appropriate for fits to the spectra of M-dwarfs.

GJ411 is the hottest dwarf in our sample. The fit to the observed spectrum is shown in Fig. 8. Within our observed spectral region the intensities of observed and computed band heads are fitted for T_{eff} = 3400 K and $\log N(C)$ = −3.48 (Fig. 8). Although the relatively poorer description of the M dwarf spectrum slope testifies to the presence of certain problems in the definition of its physical characteristics: abundances, homogeneity of atmospheres, chromospheres or other reasons (see Sect. 5).

4.1.3. Isotopic ratio $^{12}C/^{13}C$ in M dwarf atmospheres

The temperatures in M dwarf interiors are relatively low ($T < 10^6$ K), so that hydrogen burning is only possible in pp chain reactions and the hydrogen burning lifetimes are rather long (e.g. Laughlin et al. 1997). Thus despite the large convective envelopes extending down to the hydrogen burning region in a short timescales, carbon isotope abundances

Table 2. T_{eff} of our sample for solar metallicity compared with other methods: water vapour (Jones et al. 2002), infrared flux method (Tsuji et al. 1997), constant opacity (Jones et al. 1994), model fit based on temperatures derived by Leggett et al. (2000, 2001). The temperatures in italics are those derived for stars of similar spectral type.

Object	Spectral Type	T_{eff} This work	T_{eff} Water vapour	T_{eff} IRFM	T_{eff} Constant opacity	T_{eff} Model fit
GJ 411	M2V	3400	-	3510	3471	*3450*
GJ 699	M4V	3200	3300	3210	3095	3100
GJ 406	M6V	2800	3000	2800	2670	2600
VB10	M8	2600	-	2250	2506	*2250*
LHS2924	M9	2600	-	2120	2219	*2125*

Fig. 4. Top: The dependence of S on T_{eff} and log N(C). Bottom: 2600 and 2800 K synthetic spectra compared to the observed LHS2924 spectrum.

Fig. 5. Top: The dependence of S on T_{eff} and log N(C). Bottom: The best fit of synthetic spectra to the observed VB10 spectrum.

cannot be changed even in Hubble-scale times. M dwarfs are expected to preserve their initial carbon isotopes abundance from their time of formation. The situation is very different for massive ($M > 0.8 \, M_\odot$) stars, which burn hydrogen in CNO reactions and are observed to change their isotopic abundances of C, N, O. The determination of the ^{12}C/^{13}C ratio in the atmospheres of M dwarfs might provide important constraints on the theory of the evolution of the Galaxy.

We investigated the determination of the carbon isotopic ratio in the atmospheres of our observed M dwarfs. The analysis of the weak ^{13}C^{16}O bands in our comparatively low-resolution spectra of dwarfs is rather difficult (e.g., Fig. 9 for VB10). The CO band head at 2.345 is mimiced by H_2O absorption. Moreover, the overall shape of the energy distribution at these wavelengths is governed by H_2O absorption, Fig. 2. From the fit of our spectra for VB10 we can estimate the lower limit ^{12}C/^{13}C > 15. For more accurate determination using this feature it will be necessary to use spectra of better

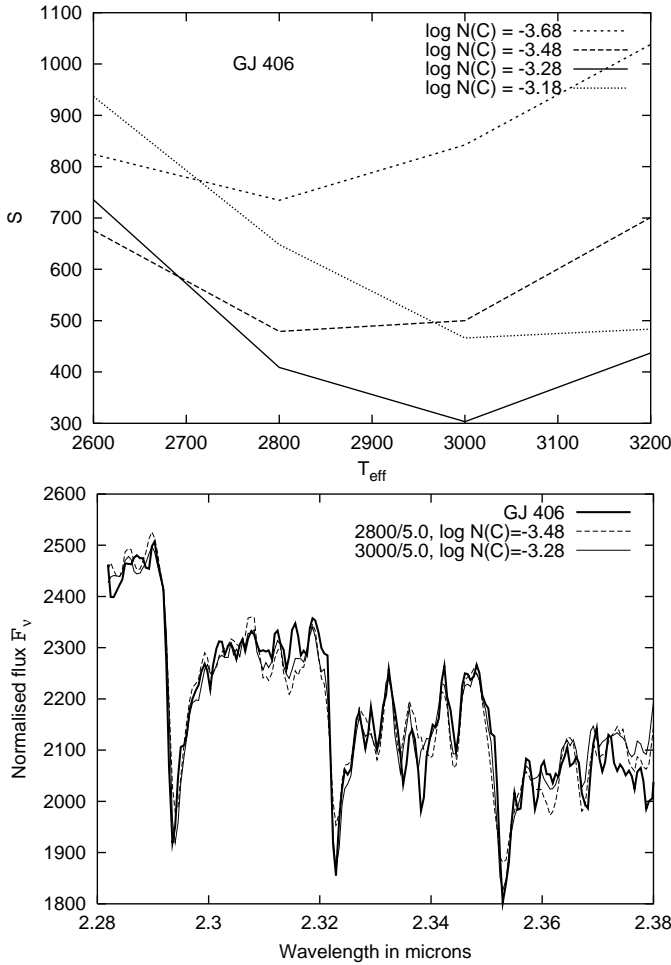**Fig. 6.** The same as in Fig. 5, but for GJ406. Synthetic spectra are shown for $T_{\rm eff}$ = 2800 and 3000 K.

Fig. 7. The same as in Fig. 5, but for GJ699. Synthetic spectra computed for 3400 and 3600 K synthetic spectra are shown.

resolution (>50 000 for ^{12}C/^{13}C in range 40–90, e.g., upper panel of Fig. 9). The other band of ^{13}C^{16}O at 2.375 μm provides a more sensitive tool for ^{12}C/^{13}C determination in M-dwarf spectra. From the fit of the observed band to our models we find ^{12}C/^{13}C $\sim$ 10. Unfortunately our confidence in this fit is weakened because our data do not extend beyond 2.38 μm. To be sure we are measuring this feature we need to have data beyond 2.38 μm. For the other M dwarfs the fits are not so good so it is necessary to confirm this result with spectra of higher resolution and signal-to-noise. Nevertheless, from the fit of our spectra we can estimate the lower limit ^{12}C/^{13}C > 10 for all stars.

4.1.4. Bands of the first overtone of CO from 4.3 to 4.6 microns

As with the $\Delta\nu$ = 2 CO bands at 2.3 μm it might be feasible to pursue the ^{12}C/^{13}C ratio using the $\Delta\nu$ = 1 CO bands at 4.4 μm. A theoretical picture of formation of the absorption features in the region of the bands of the first overtone of CO is shown in Fig. 10. Again, as for the ^{13}CO feature at 2.345 μm, lines of H_2O dominate in region (see also Fig. 2). Bands of ^{12}CO (and ^{13}CO) are actually of lower intensities relative to water.
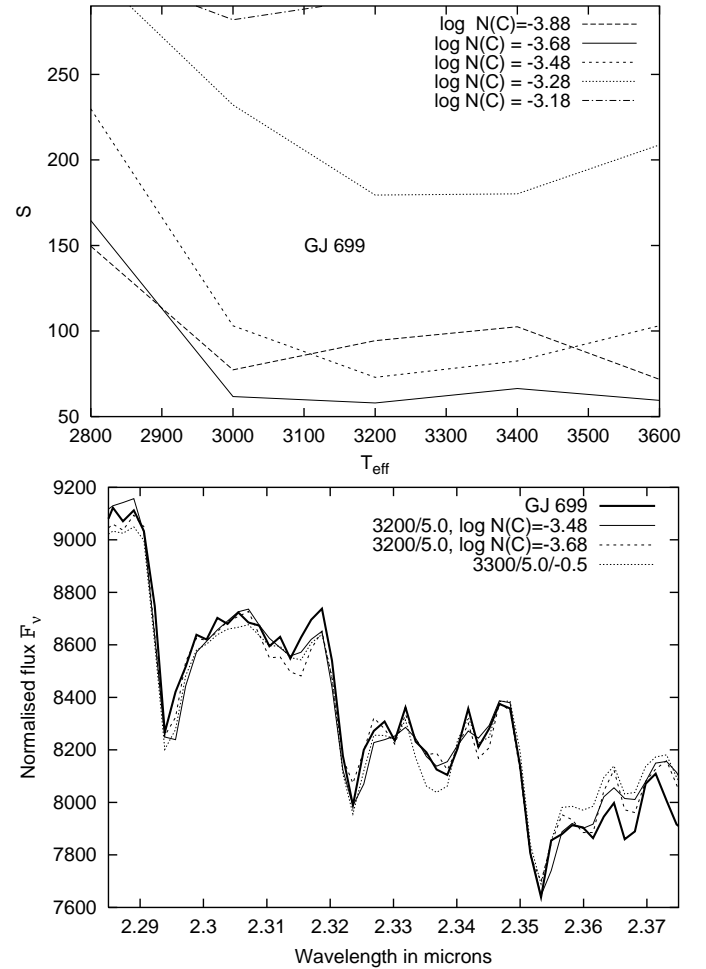
The band heads of ^{13}C fall such that their heads lie in the tails of ^{12}C bands, which are stronger. Therefore the determination of the ^{12}C/^{13}C ratio for $\Delta\nu$ = 1 CO bands is also problematic.

5. Discussion

Our effective temperature determinations are based primarily on ^{12}C^{16}O lines but also affected by H_2O lines. In Table 2 it can be seen that we find similar temperatures to those found for M dwarfs for H_2O lines alone. These results support the expected quality of the ^{12}C^{16}O and H_2O line lists.

In general, we find $T_{\rm eff}$ of our dwarfs with internal errors of around $\pm$150 K. Table 2 shows $T_{\rm eff}$ derived for M dwarfs by different methods. It indicates that whilst there is some agreement for the earlier type M dwarfs, the temperatures we derive for late spectral types are much too hot. This discrepancy arises because in the atmospheres of red dwarfs of spectral class M 6 and later (Tsuji et al. 1996; Jones & Tsuji 1997) appreciable amounts of dust forms (e.g., Tsuji 2002) that can absorb and/or scatter radiation. This dust changes the structure of model atmospheres of M dwarfs, and, hence, their spectra. The outermost layers of late M dwarf atmospheres increase due to appearance there of the "dusty" opacity. In general, we get the
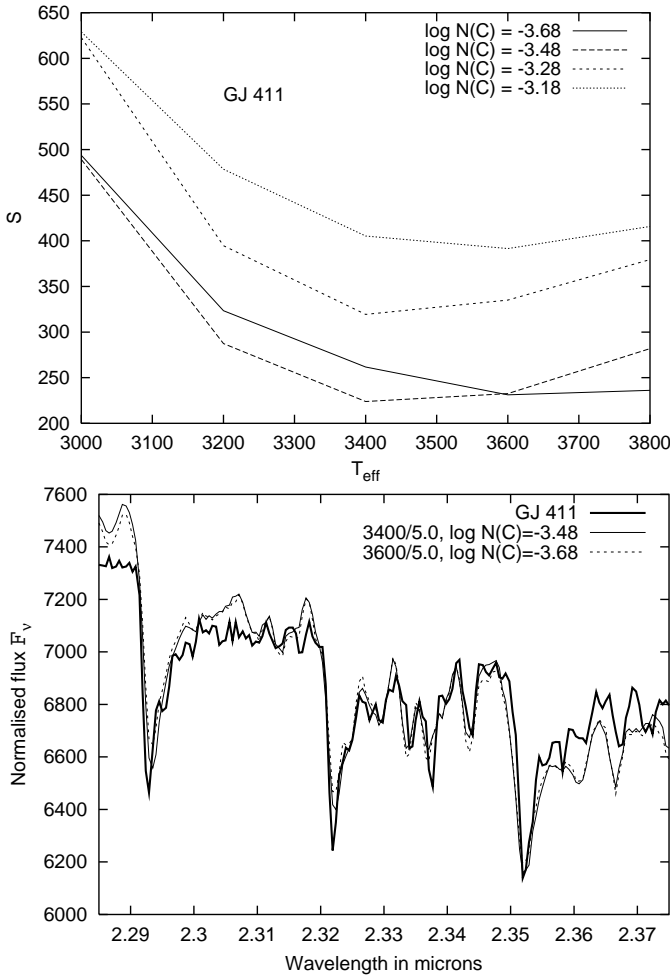
Fig. 8. The same as in Fig. 5, but for GJ411 including synthetic spectra for 3400 and 3600 K.

Fig. 9. Top: spectra computed for model atmosphere 2800/5.0, $\log N(C) = -3.28$, for $^{12}C/^{13}C = 3$ to 90 at a resolution of around 46 000. Bottom: fits of computed spectra with different $^{12}C/^{13}C$ to VB10 observed spectrum.

much more sophisticated picture of formation of late dwarf spectra in the "dusty" atmospheres in comparison with "non-dusty" case. For the case of our fits the dust in cooler stars causes the CO bands to be relatively weaker and thus best-fit by a high temperature, non-dusty model. Analysis of our data to determine reliable temperatures for VB 10 and LHS 2924 thus requires the use of dusty models. Such models are now in preparation (Pavlenko et al., in preparation).

NLTE (Non Local Thermal Equilibrium) effects provide another possible source of error. Carbon et al. (1976) investigated NLTE effects in CO lines of the fundamental systems formed in the atmospheres of stars of giant late-type spectral classes. However, they used a rather simple model of rotational-vibrational levels of CO. Furthermore they considered the model atmospheres of red giants, where the densities are much lower, than in M dwarf atmospheres. Nevertheless, they showed the possibility of NLTE effects in CO lines, formed on depths $\tau_{1\,\mu m} < 10^{-4}$. CO lines in our cases are strong, they are formed deep in the atmosphere (due to the low opacities in continuum). The formation of absorption lines of CO occurs in M dwarfs atmospheres on a background of strong H_2O absorption. The additional absorption should strengthen the thermalisation of the radiation field on CO lines.
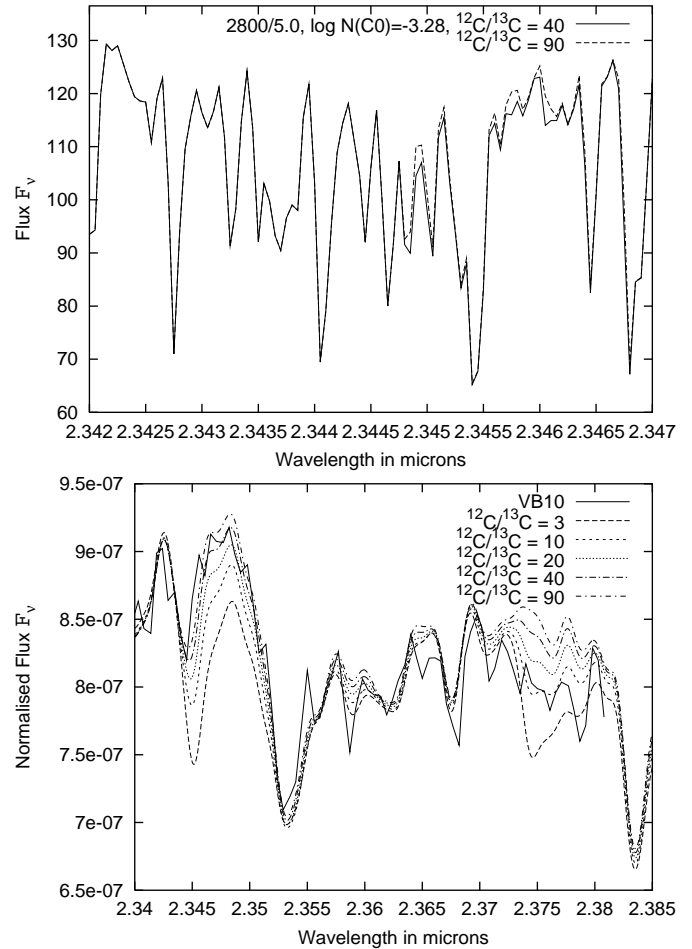
The temperature structure of M dwarf atmospheres is smoother, in comparison to the giants. Indeed, their structure is governed by convection, which "smoothes" the temperature contrast between photosphere and upper layers, which are more pronounced in atmospheres of red giants. Atmospheres of cool dwarfs are denser than giants which strengthens the thermalisation of the radiation field. All these factors should reduce NLTE effects in CO lines formed in M dwarf atmospheres. More precise estimations are possible and would be desirable when making comparisons with higher resolution data though we consider to be beyond the scope of the current work.

Our computations were carried out for model atmospheres of solar abundance. Such abundances should be prevalent for the majority M dwarfs in the vicinity of solar system. Although, our sample of M dwarfs is rather small, we have found some deviation in carbon abundances from the solar case. A more refined solution should be made using self-consistent abundances of oxygen and nitrogen.

The model atmospheres used in this work were computed in the framework of the classical assumptions by Hauschildt et al. (1999). Energy transfer in atmospheres is provided by radiation field and convection. The reliability of the computed
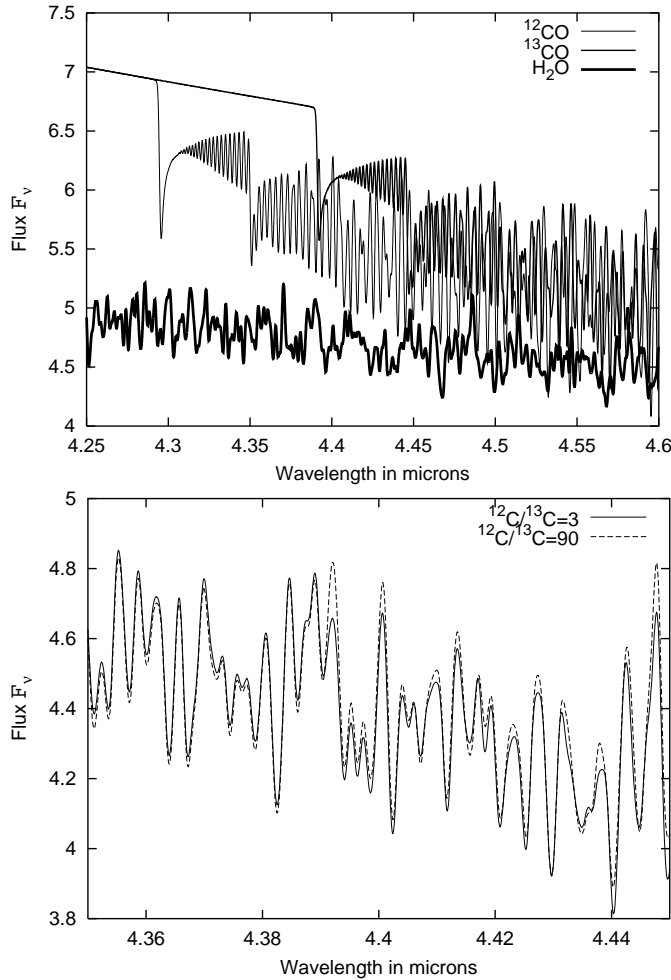
Fig. 10. Top: relative strength of $^{12}C^{16}O$, H_2O and $^{13}C^{16}O$ bands in theoretical spectrum of M-dwarf 2800/5.0/0. and a combined spectra computed for the case of $^{12}C^{16}O + H_2O$ and $^{12}C^{16}O + ^{13}C^{16}O + H_2O$ absorption. Bottom: synthetical spectra computed for 2800/5.0 model atmospheres and different $^{12}C/^{13}C$. The resolution $R = 4600$ was adopted.

model atmosphere is determined by both the completeness of the opacity sources as well as the model of convective processes (Ludwig et al. 1992). Absorption by H_2O bands determines the opacity in the infrared spectra of red stars. However, the existing line lists are not sufficiently complete (e.g., Jones et al. 2002). The CO line list used in this work was computed for solar work and so is believed to be more than adequate for the lower energy states accessed in M dwarf atmospheres (Goorvitch 1994). Overall we do not consider that incompleteness in the H_2O line lists will cause temperatures derived from CO bands to change by more than 150 K.

The spectra presented here can not be used to determine reliable $^{12}C/^{13}C$ ratios. Nonetheless we propose that with a slightly different wavelength coverage than observed for this study, the ^{13}CO feature at 2.375 μm should be a strong constraint on the $^{12}C/^{13}C$ ratio. For the other ^{13}CO feature we investigated the situation is complicated by $^{13}C^{16}O$ bands forming amongst strong H_2O absorption. One way of dealing with such "contamination" would be to obtain higher resolution

data. In the upper panel of Fig. 9 we show synthetic spectra at a resolution of around 46 000, here even at low $^{12}C/^{13}C$ ratios the ^{12}CO and ^{13}CO bands can be distinguished. We have also investigated the possible use of the 4.4–4.6 micron region. However, this region does not appear to improve the possibility of determining $^{12}C/^{13}C$.

References

Allard, F., & Hauschildt, P. 1995, ApJ, 445, 433
Allard, F., Hauschildt, P. H., & Schwenke, D. 2000, ApJ, 540, 1005
Aller, L. H., & McLaughlin, D. B. 1965, Stellar structure (The University Chigago Press, Chicago and London), 1
Baldwin, J. R., Frogel, J. A., & Persson, S. E. 1973, ApJ, 184, 427
Carbon, D. F., Milkey, R. W., & Heasley, J. N. 1976, ApJ, 207, 253
Davidge, T. J., & Boeshaar, P. C. 1993, ApJ, 403, 47L
Forbes, F. F., Stonaker, W. F., & Johnson, H. L. 1970, AJ, 75, 158
Gerardy, C. L., Fesen, R. A., Hiflich, P., & Wheeler, J. C. 2000, AJ, 119, 2968
Goorvitch, D. 1994, ApJS, 95, 535
Gurvitz, L. V., Weitz, I. V., & Medvedev, V. A. 1982, Thermodynamic properties of individual substances (Moscow Science)
Hauschildt, P., Allard, F., & Baron, E. 1999, ApJ, 512, 377
Hinkle, K. H. 1978, ApJ, 220, 210
Heasley, J. N., & Milkey, R. W. 1976, ApJ, 205, L43
Heasley, J. N., Ridgway, S. T., Carbon, D. F., Milkey, R. W., & Hall, D. N. B. 1978, ApJ, 219, 970
Jones, H. R. A., Longmore, A. J., Jameson, R. F., & Mountain, C. M. 1994, MNRAS, 267, 413
Jones, H. R. A., Longmore, A., Allard, F., & Hauschildt, P. 1996, MNRAS, 280, 77
Jones, H. R. A., & Tsuji, T. 1997, ApJ, 480, 39L
Jones, H. R. A., Pavlenko, Ya. V., Viti, S., & Tennyson, J. 2002, MNRAS, 329, 290
Kraus, M., Krugel, E., Thum, C., & Geballe, T. R. 2000, A&A, 362, 158
Martin, E. 1999, MNRAS, 302, 59
Kirkpatrick, J. D., Henry, T. J., & McCarthy, D. W. 1991, ApJS, 77, 417
Kirkpatrick, J. D., Kelly, D. M., Rieke, G. H., et al. 1993. ApJ, 402, 643
Kleinmann, S. G., & Hall, D. N. B. 1986, ApJS, 62, 501
Kupka, F., Piskunov, N., Ryabchikova, T. A., Stempels, H. C., & Weiss, W. W. 1999, A&AS, 138, 119
Lazaro, C., Lynas-Gray, A. E., Clegg, R. E. S., Mountain, M., & Zadrowny, A. 1991, MNRAS, 62
Leggett, S. K. 1992. ApJS, 82, 351
Leggett, S .K., Allard, F., Dahn, C., et al. 2000, ApJ, 535, 965
Leggett, S. K., Allard, F., Geballe, T. R., Hauschildt, P. H., & Schweitzer, A. 2001, ApJ, 548, 908

Laughlin, G., Bodenheimer, P., & Adams, F. C. 1997, ApJ, 482, 420

Ludwig, H.-G., Allard, F., & Hauschildt, P. H. 2002, A&A, 395, 99

McGregor, P. J. 1987, ApJ, 312, 195

Palla, F., Bachiller, R., Stanghellini, L., Tosi, M., & Galli, D. 2000, A&A, 355, 69

Partrige, H., Schwenke, D. J. 1997, Chem. Phys., 106, 4618

Pavlenko, Ya. V. 2000, Astron. Rept., 44, 219

Pavlenko, Ya. V. 2002, Astron. Rept., 46, 567

Pilachowski, C., Sneden, C., Hinkle, K., & Joyce, R. 1997, Metal-Poor Giants. Astron. J., 114, 819

Scott, A. D., Rawlings, J. M. C., Krautter, J., & Evans, A. 1994, MNRAS, 268, 749

Schild, H., Boyle, S. J., & Schmid, H. M. 1992, MNRAS, 258, 95

Schweitzer, A., Hauschildt, P. H., Allard, F., & Basri, G. 1996, MNRAS, 283, 821

Sneden, C., & Pilachowski, C. A. 1984, PASP, 96, 38

Suntzeff, N. B., & Smith, V. V. 1991, ApJ, 381, 160

Tsuji, T. 1973, A&A, 23, 411

Tsuji, T., Ohnaka, K., & Aoki, W. 1996, A&A, 305, 1

Tsuji, T., Ohnaka, K., & Aoki, W. 1997, ASP Conf. Ser., 124, ed. H. Okuda, T. Matsumoto, & T. Rollig, 91

Tsuji, T. 2002, ApJ, 575, 264

Viti, S., Jones, H., Maxted, P., & Tennyson, J. 2002, MNRAS, 329, 290

Unsold, A. 1955, Physik der Sternatmospheren, 2nd ed. (Springer, Berlin)